Molecular Microbiology (2009) 72(2), 410–424 ■
doi:10.1111/j.1365-2958.2009.06651.x
First published online 16 March 2009

The conserved C-terminal tail of FtsZ is required for the septal localization and division inhibitory activity of MinC^C/MinD

Bang Shen and Joe Lutkenhaus*
Department of Microbiology, Molecular Genetics and Immunology, University of Kansas Medical Center, Kansas City, KS 66160, USA.

Summary

The *Escherichia coli* Min system contributes to spatial regulation of cytokinesis by preventing assembly of the Z ring away from midcell. MinC is a cell division inhibitor whose activity is spatially regulated by MinD and MinE. MinC has two functional domains of similar size, both of which have division inhibitory activity in the proper context. However, the molecular mechanism of the inhibitory action of either domain is not very clear. Here, we report that the septal localization and division inhibitory activity of MinC^C/MinD requires the conserved C-terminal tail of FtsZ. This tail also mediates interaction with two essential division proteins, ZipA and FtsA, to link FtsZ polymers to the membrane. Overproduction of MinC^C/MinD displaces FtsA from the Z ring and eventually disrupts the Z ring, probably because it also displaces ZipA. These results support a model for the division inhibitory action of MinC/MinD. MinC/MinD binds to ZipA and FtsA decorated FtsZ polymers located at the membrane through the MinC^C/MinD–FtsZ interaction. This binding displaces FtsA and/or ZipA, and more importantly, positions MinC^N near the FtsZ polymers making it a more effective inhibitor.

Introduction

Cell division in *Escherichia coli* is mediated by a cytokinetic ring, formed by the ordered assembly of at least a dozen division proteins (Lutkenhaus, 2007). The assembly of this ring is initiated by the formation of a membrane-associated structure called the Z ring (Bi and Lutkenhaus, 1991), which consists of FtsZ polymers attached to the membrane by ZipA and FtsA, two essential membrane-associated division proteins (Hale and de Boer, 1997; Pichoff and Lutkenhaus, 2002; 2005; Lutkenhaus, 2007). ZapA and ZapB are also part of the Z ring, but are not essential (Gueiros-Filho and Losick, 2002; Ebersbach *et al.*, 2008). The Z ring functions as a scaffold for the recruitment of all other cell division proteins to make a mature cytokinetic ring capable of carrying out cytokinesis (Pichoff and Lutkenhaus, 2002; Dajkovic *et al.*, 2008a).

Both FtsA and ZipA bind to the conserved, C-terminal tail of FtsZ, which consists of approximately 15 amino acids at the extreme C-terminus (Huang *et al.*, 1996; Hale and de Boer, 1997; 1999; Wang *et al.*, 1997; Liu *et al.*, 1999; Ma and Margolin, 1999; Hale *et al.*, 2000; Haney *et al.*, 2001). Although a Z ring can form with the aid of just ZipA or FtsA, such a ring is non-functional, as other division proteins are not recruited unless both are present (Hale and de Boer, 1999; Pichoff and Lutkenhaus, 2002).

The Z ring must be accurately placed at the middle of the cell to ensure the production of equally sized progeny cells. There are two known negative regulatory systems involved in the spatial regulation of the Z-ring positioning (Rothfield *et al.*, 2005; Lutkenhaus, 2007). One system, called Noc (nucleoid occlusion), inhibits Z-ring formation over the nucleoid. This activity restricts Z-ring formation to the poles and mid-cell, which are not occupied by the nucleoid (Mulder and Woldringh, 1989; Yu and Margolin, 1999). SlmA in *E. coli* contributes to nucleoid occlusion by interacting with DNA and FtsZ directly but a detailed mechanism is not clear (Bernhardt and de Boer, 2005). The other system, called Min, blocks Z-ring formation at the cell poles (de Boer *et al.*, 1989). It consists of three components (MinC, MinD and MinE) and has been extensively studied (de Boer *et al.*, 1989); however, some aspects of its function are still not known. The combination of Min and Noc restricts Z-ring formation to the middle of the cell.

The effector of the Min system is MinC, which blocks cell division by preventing Z-ring formation (de Boer *et al.*, 1989; 1990; Bi and Lutkenhaus, 1993; Hu *et al.*, 1999). MinC requires MinD for full activity; in part, because MinD recruits MinC to the membrane (Hu and Lutkenhaus, 2001; Hu *et al.*, 2003; Lackner *et al.*, 2003). MinD is a membrane-associated ATPase which plays a central role

Accepted 22 February, 2009. *For correspondence. E-mail jlutkenh@kumc.edu; Tel. (+1) 913 588 7054; Fax (+1) 913 588 7295.

in the Min system. When bound to ATP, MinD dimerizes and binds to the membrane (Hu *et al*., 2003; Lackner *et al*., 2003). The subsequent recruitment of MinC leads to a cell division inhibitory complex (MinC/MinD) that is evenly distributed on the membrane. The activity of the MinC/MinD complex is spatially regulated by MinE, which restricts the MinC/MinD complex to the poles of the cell (de Boer *et al*., 1989). MinE does this by stimulating the pole to pole oscillation of MinC/MinD through its ability to stimulate the ATPase activity of MinD and thus, the release of MinD from the membrane (Hu and Lutkenhaus, 1999; 2001; Raskin and de Boer, 1999a,b; Fu *et al*., 2001; Hale *et al*., 2001; Hu *et al*., 2002; Shih *et al*., 2003). Such dynamic behaviour of the Min proteins results in a time-averaged concentration of the MinC/MinD division inhibitor that is highest at cell poles and lowest at mid-cell where the Z-ring forms (Meinhardt and de Boer, 2001).

Structural, sequence and functional analyses of MinC reveal that it has two domains of approximately equal size (Hu and Lutkenhaus, 2000; Cordell *et al*., 2001). Both domains are essential for MinC to spatially regulate division because mutations mapping in either domain lead to minicell formation. The *min* operon on a single copy plasmid containing the *minC-G10D* {located in the N-terminal domain [MinC$^{1–115}$ (MinC^N)]} or *minC-R172A* mutation {located in the C-terminal domain (MinC$^{116–1231}$ (MinC^C)]} has lost the ability to complement a *min* deletion strain (M. Wissel and J. Lutkenhaus, unpubl. data; Zhou and Lutkenhaus, 2005).

The two domains of MinC have been separated to determine the basis for their activity. Overproduction of a MalE-MinC^N fusion blocks Z-ring formation *in vivo* and the purified protein antagonizes FtsZ polymer assembly *in vitro* without affecting the GTPase activity of FtsZ (Hu and Lutkenhaus, 2000). The C-terminal domain of MinC mediates homodimerization and interaction with MinD. Overproduction of MinC^C alone does not affect cell division, but it has inhibitory activity in the presence of MinD (Shiomi and Margolin, 2007). *In vitro* MinC^C also limits the bundling of FtsZ filaments (Dajkovic *et al*., 2008a).

At low expression levels, green fluorescent protein (GFP)–MinC^C/MinD localizes to the Z ring without disrupting it (Johnson *et al*., 2002). This localization is dependent upon FtsZ but not other early division proteins such as FtsA, ZipA and ZapA (Johnson *et al*., 2002; 2004; Zhou and Lutkenhaus, 2005), suggesting that MinC^C/MinD interacts with FtsZ directly. An interaction between FtsZ and MinC^C/MinD was observed in an *in vitro* assay (Dajkovic *et al*., 2008a), which strongly supports this idea. In this paper we further investigate the mechanism by which MinC^C/MinD antagonizes Z-ring formation. We isolated FtsZ mutants that are resistant to MinC^C/MinD and then used these mutants to study the MinC^C/MinD–FtsZ interaction and the basis of the toxicity associated with MinC^C/MinD.

Results

Isolation of FtsZ mutants resistant to MinC^C/MinD

Overproduction of MinC^C/MinD disrupts the Z ring and causes filamentation and therefore lethality (Shiomi and Margolin, 2007). There are several lines of evidence suggesting that MinC^C/MinD binds FtsZ (Johnson *et al*., 2002; 2004; Dajkovic *et al*., 2008a). To further study the inhibitory mechanism of MinC^C/MinD, we exploited the above phenotype in a screen for FtsZ mutants that are resistant to MinC^C/MinD. To this end, we performed PCR random mutagenesis over the coding region of *ftsZ* and screened for mutants that still support division and can suppress the toxicity of MinC^C/MinD overexpression.

Using the strategy described in *Experimental procedures*, we isolated four FtsZ mutants (each was obtained multiple times) which are resistant to MinC^C/MinD. Each of these mutants contained a single mutation in *ftsZ* – either D373E, I374V, L378V or K380M (Fig. 1 and Fig. S1). Interestingly, each of these mutations result in an amino acid substitution in the C-terminal conserved tail of FtsZ that is also involved in interaction with the essential division proteins FtsA and ZipA. All four mutations, when introduced into pBANG112, do not affect its ability to complement the *ftsZ* depletion strain [S7 (*ftsZ*^{0} *recA*::Tn*10 min::kan*)/pKD3C (*ftsZ*$^+$)] at 42°C or 37°C, although the presence of the *ftsZ-L378V* mutation causes the cells to grow a little slower than the others (data not shown). As these mutations do not affect complementation of the *ftsZ* depletion strain, they must not disrupt the essential activities of FtsZ required for cell division (see below). Among the four mutants, FtsZ-I374V afforded the greatest resistance to MinC^C/MinD (Fig. S1 and data not shown) and was therefore chosen for subsequent studies. It is likely that the resistance to MinC^C/MinD afforded by all four mutations is due to the same mechanism because they map to the same small region of *ftsZ*.

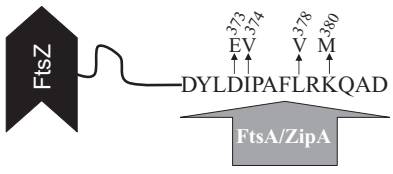

Fig. 1. Diagram of FtsZ. A cartoon of FtsZ showing the sequence of the conserved C-terminal tail involved in binding ZipA and FtsA and the location of the amino acid substitutions due to the mutations isolated in this study.

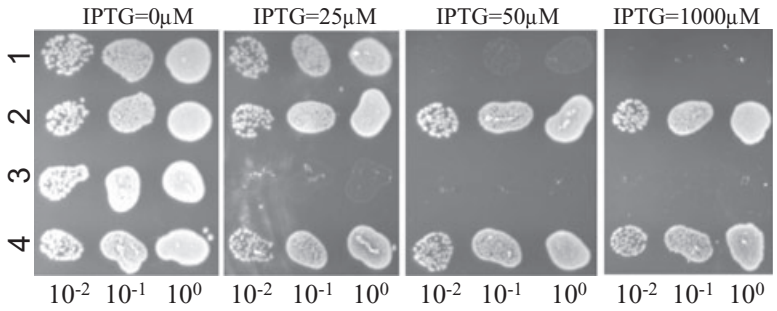

Fig. 2. FtsZ-I374V is resistant to both MinC^C/MinD and MinC/MinD. One colony of each strain was resuspended in 900 μl of LB medium and serially diluted by 10. Then 3 μl culture from each dilution was spotted on plates (with Spc) with or without IPTG (as indicated) and incubated overnight at 37°C. 1, S4/pBANG59 (*ftsZ-WT, min::kan*/P*tac::minCD*); 2, BSM374/pBANG59 (*ftsZ-I374V, min::kan*/P*tac::minCD*); 3, S4/pBANG75 (*ftsZ-WT, min::kan*/P*lac::minC^{C}D*); 4, BSM374/pBANG75 (*ftsZ-I374V, min::kan*/P*lac::minC^{C}D*).

Characterization of FtsZ-I374V mutant

Escherichia coli cells are sensitive to the FtsZ protein level because they have different morphologies with different *ftsZ* expression levels. To get a better idea about the effect of this mutation (I374V) on FtsZ function we used the lambda RED recombineering system (Datsenko and Wanner, 2000) to put the *ftsZ-I374V* mutation to the chromosome at its native locus. The resultant strain [BSZ374 (*ftsZ-I374V*)] does not show any significant difference to the control strain [S3 (*ftsZ*-WT)] in terms of growth rate and morphology. The only effect of the mutation was observed when the entire *min* locus was deleted from these strains to give BSM374 (BSZ374 *min::kan*) and S4 (S3 *min::kan*). BSM374 grew similarly to S4 at 30°C and 37°C but failed to form isolated colonies at room temperature (20°C). S4 grew at room temperature but the cells were filamentous.

BSM374 (*ftsZ-I374V, min::kan*) is resistant to MinC^C/MinD and also displays resistance to MinC/MinD. As shown in the spot test in Fig. 2, the control strain S4 (*min::kan*) containing plasmids expressing MinC/MinD (pBANG59/P*tac::minCD*) or MinC^C/MinD (pBANG75/P*lac::minC^{C}D*) under control of IPTG-inducible promoters did not grow at or above 50 μM IPTG (Fig. 2, row 1) and 25 μM IPTG (Fig. 2, row 3) respectively. Even though pBANG75 requires less IPTG to prevent the growth of the S4 strain, it is a higher copy number plasmid than pBANG59 (around 10 for pBANG75 and 1–2 for pBANG59) and has a stronger ribosome binding site for MinC^C translation (compared to MinC). As will be shown later, the minimal amount of protein required to prevent the growth of this strain is actually higher for MinC^C/MinD than for MinC/MinD. In contrast to S4 containing these plasmids, BSM374/pBANG59 (*ftsZ-I374V*, *min::kan*/P*tac::minCD*) and BSM374/pBANG75 (*ftsZ-I374V*, *min::kan*/P*lac::minC^{C}D*) could grow with IPTG as high as 1000 μM (Fig. 2, rows 2 and 4) and the cells were not filamentous. As FtsZ-I374V confers resistance to MinC/MinD in addition to MinC^C/MinD, it is surprising to note that the BSZ374 cells have wild-type (WT) morphology and produce very few minicells. We expected it might produce minicells at a frequency comparable to a *min* null strain because FtsZ-I374V displays some resistance to MinC/MinD. Deletion of the *min* locus in BSZ374 did result in a minicell phenotype indicating that FtsZ-I374V could produce polar rings and lead to polar divisions when Min was absent. These observations suggest that FtsZ-I374V still responds to MinC/MinD to some extent and the polar Z rings made from FtsZ-I374V are still susceptible to MinC/MinD (discussed later).

To rule out the possibility that the MinC/MinD resistance of BSZ374 (*ftsZ-I374V*) is due to an increased steady-state protein level or reduced GTPase of the mutant protein, we checked the SulA sensitivity of this strain. SulA is another cell division inhibitor (Bi and Lutkenhaus, 1993) and it is well documented that increased FtsZ or FtsZ mutants with decreased GTPase activity confer resistance to SulA (Lutkenhaus *et al*., 1986; Dai *et al*., 1994; Dajkovic *et al*., 2008b). A careful spot test revealed that the SulA sensitivity of the BSZ374 (*ftsZ-I374V*) strain was identical to that of the WT strain S3 (data not shown). This indicates that the protein level and GTPase of this mutant FtsZ are not significantly affected by the mutation.

Interaction of FtsZ I374V with FtsA and ZipA

Previously, a yeast-two-hybrid assay (YTH) showed that the conserved extreme C-terminus of FtsZ containing the I374 residue was involved in the FtsZ–FtsA and FtsZ–ZipA interactions (Haney *et al*., 2001). Here, we asked whether the *ftsZ-I374V* mutation affected these interactions. Using the YTH system to look at these interactions, we found that FtsZ-I374V interacted with ZipA similarly to WT FtsZ but failed to interact with FtsA (Table S1). The loss of the interaction between FtsZ-I374V and FtsA in this assay is somewhat surprising

because FtsZ-I374V can fully complement the *ftsZ* depletion strain and support cell division. We therefore examined the effect of the *ftsZ-I374V* mutation on the recruitment of FtsA to the septum by immunofluorescent microscopy.

Immuno-staining of cells from exponentially growing cultures revealed that Z rings were present at similar frequencies in BSZ374 (*ftsZ-I374V*) and the WT strain S3 (> 80% of cells had a Z ring at midcell; no polar rings were observed). FtsA and ZipA were both efficiently recruited to the Z ring in BSZ374 (*ftsZ-I374V*) because FtsA rings and ZipA rings were observed at similar frequencies (> 80%) to Z rings (Table S2). The ability of ZipA and FtsA to localize to Z rings in the FtsZ-I374V mutant strain was also investigated by using GFP fusions as reported previously (Pichoff and Lutkenhaus, 2001; 2007). Although these fusions cause filamentation, at appropriate induction levels both ZipA-GFP and GFP-FtsA formed ring structures in FtsZ-I374V cells that were similar to those in WT cells (Fig. S2), indicating that both of these fusions localized to the Z ring. The results of the FtsA localization appear inconsistent with the YTH result. It is possible, however, that there is an interaction between FtsZ-I374V and FtsA that is sufficient to recruit FtsA to the Z ring even though it cannot be detected by YTH.

FtsZ-I374V is unable to recruit MinC^C/MinD in vivo

MinC^C/MinD has been shown to localize to the Z ring as revealed by GFP-tagging of MinC^C (Johnson *et al*., 2002; Zhou and Lutkenhaus, 2005). Several lines of evidence suggest that MinC^C/MinD interacts with FtsZ directly to achieve this localization (Johnson *et al*., 2002; 2004; Dajkovic *et al*., 2008a). Our results are consistent with this idea because we isolated FtsZ mutants that are resistant to MinC^C/MinD. We speculated that the MinC^C/MinD resistance of these mutants is due to the loss of interaction with MinC^C/MinD. To test this hypothesis, we first checked the ability of GFP–MinC^C/MinD to localize to the Z ring. We introduced a plasmid (pHJZ109) expressing GFP–MinC^C/MinD under an IPTG-inducible promoter control into FtsZ-WT and FtsZ-I374V strains [the GFP fusion used here is distinct from the GFP–MinC$^{122–2231}$ construct described in Shiomi and Margolin (2007) because it does not interfere with the activity of MinC^C]. GFP–MinC^C/MinD expression was induced with IPTG and fluorescence was monitored over time. As shown in Fig. 3, the localization of GFP–MinC^C/MinD to the Z ring in the S4 (*ftsZ-WT*, *min::kan*) strain was already observed before induction (Fig. 3, A1), indicating the basal expression was sufficient to allow visualization of fluorescent rings. The GFP–MinC^C/MinD rings became brighter (Fig. 3, A2) after 40 min of induction; however, as the induction time increased further, the GFP–MinC^C/MinD rings gradually disappeared indicating that the Z rings were being disrupted. At 70 min after induction, cells were longer and only a small fraction still possessed GFP–MinC^C/MinD rings (Fig. 3, A3); in most filaments the GFP–MinC^C/MinD was primarily on the membrane but was also in spiral-like structures in many cells. At 100 min of induction, all cells became filamentous and no GFP–MinC^C/MinD rings were observed (Fig. 3, A4). These results are consistent with previously reported observations that GFP–MinC^C/MinD is able to localize to the Z ring but that high levels disrupt the Z ring causing filamentation (Johnson *et al*., 2002; Shiomi and Margolin, 2007). In contrast, when GFP–MinC^C/MinD was induced in the FtsZ mutant strain BSM374 (*ftsZ-I374V min::kan*), cells never became filamentous and GFP–MinC^C/MinD never localized as a ring but was evenly distributed on the membrane at both early and late times after induction (Fig. 3B). These observations strongly indicate that FtsZ-I374V does not interact with MinC^C/MinD.

FtsZ-I374V does not bind MinC^C/MinD in vitro

To confirm the loss of interaction between FtsZ-I374V and MinC^C/MinD, we employed an *in vitro* recruitment assay described previously (Dajkovic *et al*., 2008a) to assess the interaction between FtsZ and MinC^C/MinD. In this assay FtsZ-WT polymers that are assembled in the presence of GMPCPP are efficiently recruited to vesicles to which MinD and MinC^C are bound. MinD binds to phospholipid vesicles (multilamellar vesicles: MLVs) in an ATP-dependent manner and this MinD–MLV complex is readily sedimented in a tabletop centrifuge. If MinC^C is added to the reaction, it is recruited to the MinD–MLV complex due to the interaction between MinC^C and MinD. If WT FtsZ is polymerized with GMPCPP and included in the reaction with MinD+ATP, MinC^C and MLVs, the FtsZ polymers are recruited to the vesicle–Min complex (Fig. 4A, lane 6). This recruitment requires MinC^C as FtsZ polymers are not sedimented when MinC^C is not included (Fig. 4A, lane 2). Also, unpolymerized FtsZ is not recruited to the MinC^C/MinD–vesicle complex (Fig. 4A, lane 4). These results demonstrate that the centrifugation forces used here are insufficient to pellet FtsZ polymers not bound to vesicles and that there is a direct interaction between the MinC^C/MinD complex and FtsZ. We then purified the FtsZ-I374V protein and tested its ability to bind MinC^C/MinD using the above recruitment assay. Preliminary results revealed that the FtsZ-I374V protein displayed identical polymerization properties to WT FtsZ; both polymerized with GTP and GMPCPP and not GDP (Fig. S3). When used in the recruitment assay, FtsZ-I374V polymers did not bind to the MinC^C/MinD–phospholipid vesicle complex (Fig. 4B, lane 6), confirming that FtsZ-I374V does not interact with MinC^C/MinD.

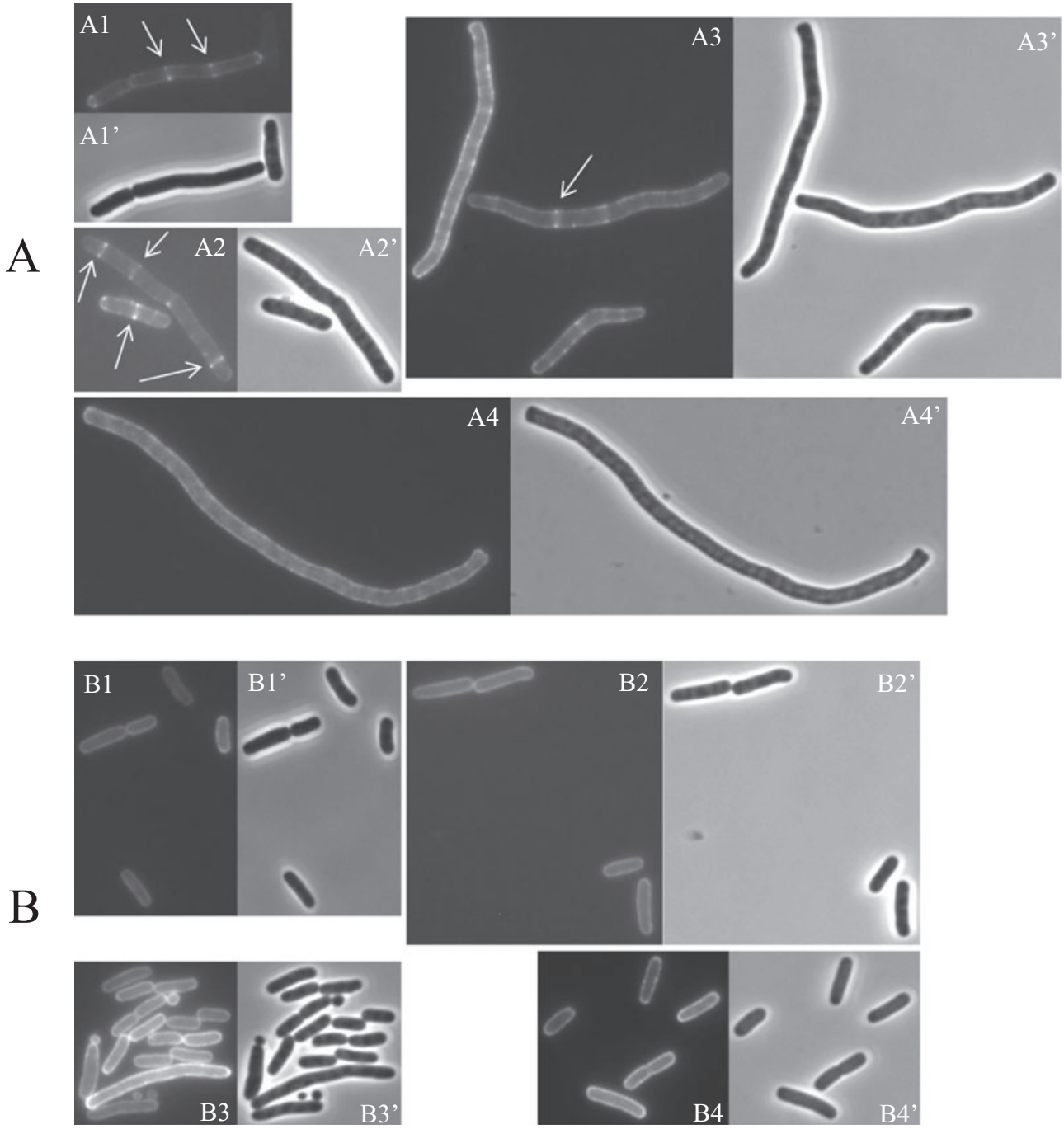

Fig. 3. GFP–MinC^C/MinD does not localize to Z rings composed of FtsZ-I374V. Expression of GFP–MinC^C/MinD was induced with IPTG in S4/pHJZ109 (*ftsZ-WT, min::kan*/P*lac::gfp-minC^C D*) (A) and BSM374/pHJZ109 (*ftsZ-I374V, min::kan*/P*lac::gfp-minC^C D*) (B) and samples at various times were subjected to fluorescent microscopy. Fluorescence micrographs (A1-A4, B1-B4) and the corresponding phase contrast images (A1′–A4′, B1′–B4′) showing the localization of GFP–MinC^C/MinD over time in these two strains are presented. Cells were grown in the presence of 50 μM IPTG at 37°C for 0 min (A1, B1), 40 min (A2, B2), 70 min (A3, B3) and 100 min (A4, B4). Arrows in A indicate GFP–MinC^C/MinD localized to rings. The contrast and brightness of these pictures are adjusted unequally for better viewing.

FtsZ-I374V is still sensitive the N-terminus of MinC

MinC has two functional domains and each domain affects FtsZ function but the mechanism of action is quite different (Hu *et al*., 1999; Hu and Lutkenhaus, 2000; Shiomi and Margolin, 2007; Dajkovic *et al*., 2008a). Although FtsZ-I374V confers resistance to MinC/MinD we speculated that it only suppresses the action of MinC^C and

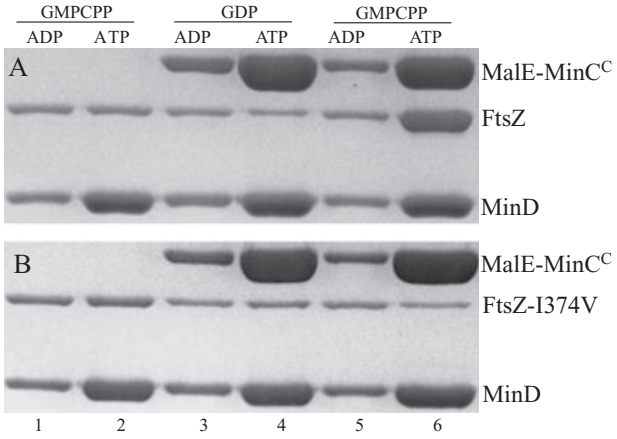

Fig. 4. FtsZ-I374V does not bind MinC^C/MinD *in vitro*. The interaction between FtsZ and MinC^C/MinD was determined by a sedimentation assay in which the recruitment of FtsZ polymers to a phospholipid vesicle-associated MinC^C/MinD complex was assessed. Reactions containing multilamellar phospholipid vesicles (MLV, 400 μg ml^{-1}), MinD (6 μM), WT FtsZ (A) or FtsZ-I374V (B) at 6 μM, GMPCPP or GDP (200 μM) with (lane 3–6) or without (lanes 1 and 2) MalE-MinC^C (6 μM) were incubated at room temperature for 5 min in ATPase buffer [25 mM Tris-HCl (pH 7.5), 50 mM KCl and 5 mM $MgCl_2$). ATP or ADP (1 mM) was then added to the reactions and incubated for another 5 min. The reactions were then centrifuged at 10 000 *g* for 2 min. The pellets were solubilized and analysed by SDS-PAGE.

is still sensitive to MinC^N. To test this we introduced a plasmid (pZH111) expressing a MalE-MinC^N fusion under arabinose promoter control into the S4 (*min::kan*) and BSM374 (*ftsZ-I374V min::kan*) strains to determine their sensitivity to arabinose. Neither S4 nor BSM374 containing the plasmid pZH111 (P*ara::malE-minC^N*) formed colonies on plates containing 0.2% arabinose (data not shown). Colony formation was rescued by introduction of a point mutation (G10D) in MinC^N [this mutation disrupts the activity of MinC^N (Hu *et al.*, 1999)] confirming that MinC^N was responsible for the toxicity. At low arabinose concentrations, pZH111 caused filamentation in both strains and no difference in arabinose sensitivity was detected. When grown on plates with 0.05% arabinose for 5 h, both S4/pZH111 and BSM374/pZH111 became extremely filamentous (Fig. 5A and B). This filamentation phenotype was not observed if the G10D substitution was present in MinC^N (Fig. 5A′ and B′). These observations indicate that the FtsZ-I374V mutant is as sensitive to MinC^N as the WT strain.

In the above assay MalE-MinC^N is not on the membrane, although it is still toxic if sufficiently overexpressed. To test the MinC^N sensitivity of the WT and FtsZ-I374V mutant strains under more physiological conditions, we compared the sensitivity of these two strains to MinC-R172A/MinD. The division inhibitory activity of this mutant form of MinC/MinD is from the N-terminal domain of MinC as the inhibitory activity of the C terminal domain (and its ability to localize to the Z ring) is abolished by the R172A mutation (Zhou and Lutkenhaus, 2005). As shown in Fig. 6A rows 2 and 5, the growth of both S4 (*min::kan*) and BSM374 (*ftsZ-I374V, min::kan*) bearing the plasmid (pBANG78-R172A) expressing MinC-R172A/MinD under *lac* promoter control was blocked at similar IPTG concentrations (20 μM for S4 and 30 μM for BSM374, data not shown). A Western blot showed that a similar level of the MinC-R172A protein (with MinD) was required to cause uniform filamentation in these two strains in liquid cultures

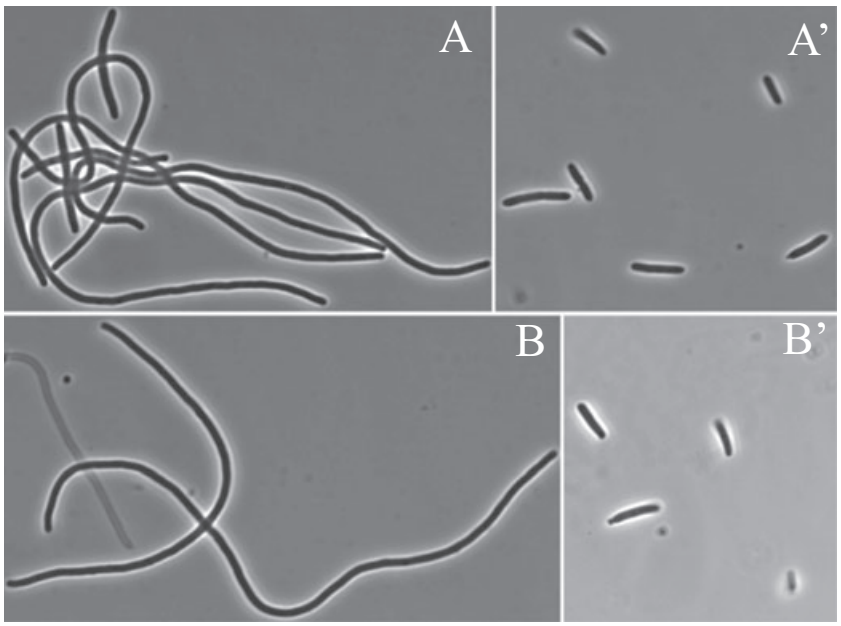

Fig. 5. The FtsZ-I374V mutant strain is sensitive to MinC^N. (A) BSM374 (*ftsZ-I374V, min::kan*) and (B) S4 (*min::kan*) harbouring the plasmid pZH111 (P*ara*::*malE-minC^N*) were grown on plates containing 0.05% arabinose at 37°C. The morphology of these cells was then checked at 5 h by phase contrast microscopy. As a control, a point mutation (G10D) that inactivates MinC^N was introduced into pZH111 and the mutant protein was expressed in BSM374 (A′) and S4 (B′) with the above conditions.

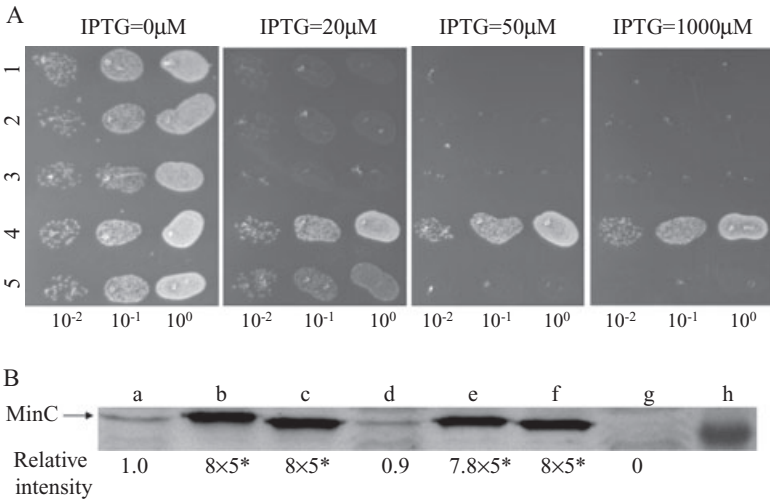

Fig. 6. Comparison of the killing efficiency of MinC/MinD and its mutants in FtsZ-WT and FtsZ-I374V strains.
A. Plasmid pBANG78 (P*lac::minCD*), pBANG78-G10D (*minC-G10D* on pBANG78) or pBANG78-R172A (*minC-R172A* on pBANG78) was transformed into S4 (*min::kan*) or BSM374 (*ftsZ-I374V, min::kan*). A spot test was done following the protocol described in Fig. 2 with the following samples: row 1: S4/pBANG78-G10D; 2: S4/pBANG78-R172A; 3: BSM374/pBANG78; 4: BSM374/pBANG78-G10D; 5: BSM374/pBANG78-R172A.
B. The minimal amount of MinC or MinC mutant proteins to cause uniform filamentation in S4 and BSM374 strains. Plasmid pBANG78 (pBANG59/P*tac::minCD* in the case of sample d) and its derivatives containing the *minC-G10D* or *minC-R172A* mutations were induced with minimal concentrations of IPTG to cause uniform filamentation in the indicated strains in liquid culture. The MinC protein level was determined by immunoblot with the WT strain S3 and Δ*min* strain S4 as controls: a: S3; b: S4/pBANG78-G10D; c: S4/pBANG78-R172A; d: S4/pBANG59; e: BSM374/pBANG78; f: BSM374/pBANG78-R172A; g: S4; h: marker at 28.8 kDa. The relative protein levels were indicated. *Loading volume for samples a, d and g was fivefold more than that of samples b, c, e and f (see *Experimental procedures*).

(Fig. 6B, lanes c and f), suggesting similar sensitivity of both strains. We also tested the sensitivity of FtsZ-WT and FtsZ-I374V to MinC^N*in vitro*. Sedimentation of both WT FtsZ and FtsZ-I374V in the presence of GTP was prevented by MalE-MinC^N in a concentration-dependent manner (data not shown). Together, these results demonstrate that FtsZ-I374V and FtsZ-WT have similar sensitivity to MinC^N. Therefore, we conclude that the MinC/MinD resistance of FtsZ-I374V is due to the resistance to MinC^C/MinD.

Concentration-dependent effect of MinC^C/MinD on Z rings

Overproduction of MinC^C in the presence of MinD inhibits assembly of Z rings (Shiomi and Margolin, 2007) even though MinC^C does not affect the polymerization of FtsZ *in vitro* (Hu and Lutkenhaus, 2000). MinC^C was shown to block the lateral association of FtsZ polymers *in vitro* and this activity may be responsible for the disruption of the Z ring *in vivo* (Dajkovic *et al.*, 2008a). However, the importance of lateral interactions between FtsZ polymers in Z-ring assembly remains enigmatic because of the relatively short length of the FtsZ protofilaments and a failure to observe multistranded polymers at division sites by electron cryotomography (Chen and Erickson, 2005; Li *et al.*, 2007). Our finding that the septal localization and division inhibitory action of MinC^C/MinD require the region of FtsZ that is also involved in the interaction with FtsA and ZipA raised the possibility that MinC^C/MinD could compete with FtsA and ZipA. Such competition could disrupt the Z ring by dislodging FtsZ polymers from the membrane.

There are at least two discrete steps in the inhibition of cell division by MinC^C/MinD. We had already observed that limited induction of GFP–MinC^C/MinD caused filamentation, but the fluorescence was present in ring structures (Fig. S4, A1). This result indicated that Z rings were present but they did not support division: the limited expression of GFP–MinC^C/MinD prevented Z-ring function without disrupting its formation. Induction of GFP–MinC^C/MinD at a higher level resulted in filamentation and initial localization to Z rings (Fig. S4, B1) which eventually disappeared (Fig. S4, B2). We reasoned that one possible mechanism by which MinC^C/MinD could block Z-ring function is to preferentially displace either FtsA or ZipA from the Z ring. If MinC^C/MinD competes more efficiently with one of the two (FtsA or ZipA) for interaction with FtsZ, then overproduction of MinC^C/MinD at some level could displace just one of them and not disrupt the ring because the Z ring can form with either FtsA or ZipA (Pichoff and Lutkenhaus, 2002).

To test this, we did immuno-staining to examine the localization of FtsZ, FtsA, ZipA and FtsK proteins in cells over-expressing MinC^C/MinD. The localization pattern of FtsK serves as an indicator of the integrity of the Z ring because its septal localization requires FtsZ, FtsA and

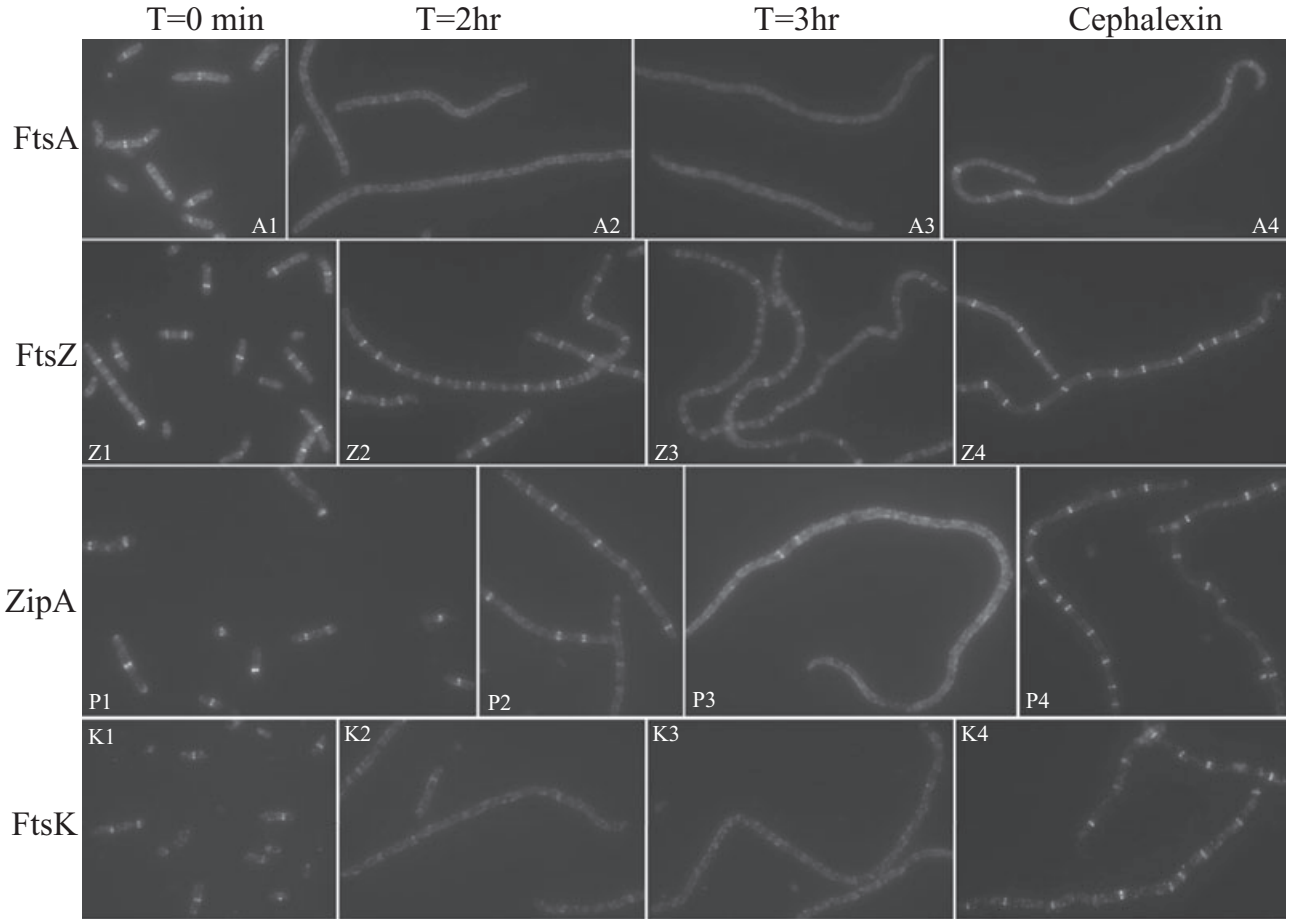

Fig. 7. Effect of MinC^C/MinD induction on the localization of FtsZ, FtsA, ZipA and FtsK. MinC^C/MinD was induced with 100 μM IPTG in S4/pBANG75 (*ftsZ-WT, min::kan*/P*lac::minC*^{C} *D*). Cells were removed at indicated time points and analysed by immunofluorescent microscopy using antisera against FtsA (A1-A3), FtsZ (Z1-Z3), ZipA (P1-P3) and FtsK (K1-K3). As a control, S4/pBANG75 cells were treated with cephalexin at 20 μg ml^{-1} for 2 h to generate filamentous cells. The localization of FtsA (A4), FtsZ(Z4), ZipA(P4) and FtsK(K4) in these filaments was also checked by immuno-staining.

ZipA (Wang and Lutkenhaus, 1998; Pichoff and Lutkenhaus, 2002). MinC^C/MinD was induced in strain S4/pBANG75 (*min::kan*/P*lac*::*minC*^{C}*D*) with 100 μM IPTG, which is sufficient to cause filamentation and prevent colony formation. At different time points samples were taken and stained using antisera against FtsZ, FtsA, ZipA and FtsK.

Before IPTG induction (Fig. 7, T = 0 min), most cells had FtsZ and ZipA rings and slightly less contained FtsA and FtsK rings. After 1 h induction, most cells still had FtsZ and ZipA rings but only a small portion of the cells had FtsA and FtsK rings (data not shown). Two hours after induction, cells were filamentous but the vast majority contained FtsZ and ZipA rings throughout their length (Fig. 7, Z2 and P2). In contrast, FtsA and FtsK rings were only rarely observed (Fig. 7, A2 and K2). By 3 h, ring localization of all four proteins was lost (Fig. 7, T = 3 h) although FtsZ and ZipA rings were sporadically observed (Fig. 7, Z3 and P3). Interestingly at this time point, FtsZ was present in spiral and ladder-like structures instead of rings. These spiral structures were also observed in other experiments using either GFP–MinC^C/MinD or FtsZ-GFP in the presence of overexpressed MinC^C/MinD, but only at specific time points. We think these structures are due to the spiraling-out of FtsZ polymers (possibly attached to the membrane through interaction with MinC^C/MinD) as Z rings are disrupted.

The change in the localization pattern of these proteins upon MinC^C/MinD induction is not due to filamentation per se, as filamentous cells of S4/pBANG75 generated by cephalexin treatment contained all four proteins in ring structures (Fig. 7, cephalexin) although FtsA and FtsK rings were present at a slightly lower number per filament. As another control MinC^C/MinD was induced in BSM374 (*ftsZ-I374V*, *min::kan*/pBANG75). The cells did not filament and FtsZ, FtsA, ZipA and FtsK formed rings at similar frequencies at all time points (data not shown). This failure of MinC^C/MinD to cause filamentation or affect

the frequency of these rings in this strain is consistent with the failure of MinC^C/MinD to bind to FtsZ-I374V and compete with FtsA and ZipA.

These results clearly demonstrate that overproduction of MinC^C/MinD initially displaces FtsA, and therefore FtsK (and presumably other downstream proteins), from the WT Z ring. Later, this overproduction eventually disrupts the Z ring, probably because it also displaces ZipA. This result provides an explanation for the earlier observation that at a low induction level GFP–MinC^C/MinD prevented division but still localized to rings (Fig. S4, A1); FtsA was displaced but Z rings still formed with the aid of ZipA. Also, the reduced frequency of FtsA rings (and FtsK rings) in S4/pBANG75 at T = 0 min (Fig. 7, T = 0 min) and in cephalexin-treated cells (Fig. 7, cephalexin) is likely due to the basal expression of MinC^C/MinD from pBANG75, because S4 and BSM374 contained FtsA rings at a similar frequency in the absence of this plasmid (Fig. S2 and data not shown).

Relative division inhibitory activity of the two domains of MinC

In the proper context both the N- and the C-terminal domains of MinC have division inhibitory activity; however, the relative efficiency of the two domains and their contribution to the activity of full-length MinC/MinD have not been determined. Previous studies have shown that when MinD is not present, MalE-MinC^N is a more potent division inhibitor than MalE-MinC^C (Hu and Lutkenhaus, 2000). The division inhibitory activity of MinC^C is only observed in the presence of MinD (Shiomi and Margolin, 2007). To compare the activity of the two domains of MinC in the same context and under more physiological conditions, we took advantage of the two MinC mutants (MinC-G10D and MinC-R172A) described previously (Hu *et al*., 1999; Zhou and Lutkenhaus, 2005). The *minC-G10D* and *minC-R172A* mutations significantly reduce the activity of MinC^N and MinC^C respectively, so that the division inhibitory activity of MinC-G10D/MinD is mainly from the MinC^C domain and that of MinC-R172A/MinD is mainly from the MinC^N domain. As shown in Fig. 6A (rows 1 and 2), the two MinC mutants displayed very similar ability to prevent the growth of the FtsZ-WT Δ*min* strain (S4) when expressed with MinD under *lac* promoter; no growth at or above 20 μM IPTG. Western blot analysis further confirmed that the same amount of the mutant MinC proteins was required to cause uniform filamentation in liquid culture (Fig. 6B, b & c).

The killing efficiency of the two MinC mutants must be significantly lower than WT MinC because WT MinC/MinD on the same vector (pBANG78/P*lac::minCD*) could not be transformed into the S4 strain (data not shown). However, another plasmid (pBANG59/P*tac::minCD*) with lower expression of MinC/MinD could be transformed into S4 (Fig. 2, row 1). Western analysis of this strain (S4/pBANG59) indicated that the minimal MinC level required to cause uniform filamentation was slightly less than the MinC level expressed from the chromosome of a WT strain (Fig. 6B, lanes d and a respectively), consistent with what was reported before (Zhou and Lutkenhaus, 2005). Comparison of the protein levels also indicates that about 40 times more mutant MinC (MinC-G10D or R-172A) was required to cause uniform filamentation in S4 (Δ*min*) strain than WT MinC (Fig. 6B, b–d and data not shown), suggesting that each domain of MinC is at least 40-fold less active than full-length MinC in blocking division.

We also wanted to compare the effect of the *ftsZ-I374V* mutation with that of the *minC-R172A* mutation to see whether they are equivalent in affecting the responsiveness of FtsZ to MinC/MinD. Both mutations eliminate the toxicity of MinC^C/MinD and therefore should have a similar effect. To do this, under the control of an IPTG-inducible promoter, WT MinC/MinD was expressed in BSM374 (*ftsZ-I374V, min::kan*) and MinC-R172A/MinD was expressed in S4 (*ftsZ-WT*, *min::kan*) and the IPTG sensitivity of these two strains was compared. As shown in Fig. 6A rows 2 and 3, growth of both strains was inhibited at the same IPTG concentration (20 μM). Subsequent analysis showed that very similar amount of MinC protein was required for WT MinC/MinD to cause filamentation in BSM374 (Fig. 6B, lane e) as for MinC-R172A/MinD to cause filamentation in the S4 strain (Fig. 6B, lane c). Thus, WT MinC/MinD has the same toxicity in the FtsZ-I374V strain as MinC-R172A/MinD has in FtsZ-WT strain. This result confirms that FtsZ-I374V is resistant to MinC^C/MinD. Consistent with this conclusion, MinC-R172A/MinD is as toxic (Fig. 6A, row 5; 6B, lane f) as WT MinC/MinD in the FtsZ-I374V strain. Also, MinC-G10D/MinD did not show any detectable toxicity in BSM374 (*ftsZ-I374V*, *min::kan*) (Fig. 6A, row 4). This latter result was expected because the inhibitory activity of both domains of MinC would be abolished.

We also used GFP–MinC/MinD and the corresponding mutants (GFP–MinC-G10D and GFP–MinC-R172A) in JS964 (Δ*min*) strain to assess the relative toxicity of the two domains of MinC and to compare them to WT MinC. The results were similar to what was shown above with untagged proteins – the two mutant forms of MinC/MinD have very similar division inhibitory activity and are 40-fold less active than WT MinC/MinD (data not shown).

Discussion

In *E. coli* and many other bacteria, the Min system contributes to the spatial regulation of cell division by inhibiting Z-ring formation near the poles of the cell (de Boer

et al., 1989). The Min system has been studied for almost 20 years and many fascinating aspects of it have been described; however, a detailed mechanism of its function is not known. The effector of the Min system is MinC, an inhibitor of Z-ring formation and, therefore cytokinesis (de Boer *et al*., 1989; 1990; Bi and Lutkenhaus, 1993; Hu *et al*., 1999). MinC is composed of two domains with distinct functions and both domains have division inhibitory activity when overexpressed: $MinC^N$ blocks Z-ring formation *in vivo* and disrupts FtsZ polymer assembly *in vitro* as assayed by sedimentation (Hu and Lutkenhaus, 2000); $MinC^C$ does not affect FtsZ sedimentation but decreases filament bundling and can localize to Z rings and block cell division when MinD is present (Hu and Lutkenhaus, 2000; Shiomi and Margolin, 2007). The detailed mechanism of the inhibitory activity of each domain is not fully understood. In the present study, we found that localization of $MinC^C$/MinD to the Z ring requires the C-terminal conserved tail of FtsZ, an unstructured region which also interacts with FtsA and ZipA (Liu *et al*., 1999; Ma and Margolin, 1999; Haney *et al*., 2001). $MinC^C$/MinD efficiently displaces FtsA on the Z ring and can therefore block the function of the Z ring; further overproduction of $MinC^C$/MinD eventually disrupts the Z ring, probably because it also displaces ZipA.

Localization of $MinC^C$/MinD to the Z ring

$MinC^C$/MinD has been shown to localize to the Z ring and this localization depends on $MinC^C$ because a point mutation (R172A) in $MinC^C$ prevents localization of GFP–$MinC^C$/MinD (Zhou and Lutkenhaus, 2005; Johnson *et al*., 2002). However, the component(s) of the Z ring that is directly involved in recruiting $MinC^C$/MinD to the septum was not clearly demonstrated even though there are several lines of evidence suggesting that it is FtsZ: (i) localization of $MinC^C$/MinD does not require other known components of the Z ring (FtsA, ZapA or ZipA) (Johnson *et al*., 2004); and (ii) direct interaction between FtsZ and $MinC^C$ has been detected in several assays (Dajkovic *et al*., 2008a). Our results strongly support that FtsZ directly recruits $MinC^C$/MinD to the septum because we isolated FtsZ mutants that are resistant to $MinC^C$/MinD, the one we studied in detail – FtsZ-I374V fails to recruit $MinC^C$/MinD to the septum, and does not interact with it *in vitro*.

The role of MinD is still not clear as the targeting of $MinC^C$/MinD to the Z ring is generally thought to be mediated by the FtsZ–$MinC^C$ interaction (Dajkovic *et al*., 2008a). However, $MinC^C$ is not targeted, nor does it have toxicity in the absence of MinD (Johnson *et al*., 2002; Shiomi and Margolin, 2007) and there is no evidence to show that MinD contacts any septal components directly. This is in contrast to DicB, a phage-encoded protein that can also target $MinC^C$ to the Z ring, but does so via an interaction with ZipA. In this case the localization is thought to be a bipartite signal involving both DicB and $MinC^C$ making contacts with ZipA and FtsZ respectively (Johnson *et al*., 2004). We examined the targeting of $MinC^C$/DicB to the Z ring in BSM374 (*ftsZ-I374V*, *min::kan*) strain by GFP tagging of $MinC^C$ and found that GFP–$MinC^C$/DicB was still targeted to the Z rings. Consistent with this, and unlike the resistance to MinC/MinD (Fig. 2), BSM374 does not show significant resistance to MinC/DicB (data not shown). This is perhaps not very surprising because of the difference in targeting of $MinC^C$ to the Z ring by MinD and DicB as discussed above. In addition, FtsZ is targeted by $MinC^C$/MinD or $MinC^C$/DicB complexes and not $MinC^C$ alone. In this sense, it is not surprising if the requirements for FtsZ to recognize these two complexes are not the same because the complexes are different. This may explain why FtsZ-I374V blocks the targeting of $MinC^C$/MinD but not $MinC^C$/DicB.

One role for MinD is to recruit and concentrate $MinC^C$ on the membrane but there is more, because MinD greatly enhances the toxicity of a version of $MinC^C$ ($MinC^C$-MTS) which is targeted to the membrane artificially by addition of a membrane targeting sequence (B. Shen and J. Lutkenhaus, unpubl. data). $MinC^C$-MTS does not show detectable toxicity in the absence of MinD but becomes a potent division inhibitor when MinD is present. This observation is similar to what was observed previously with full-length MinC (Johnson *et al*., 2002). Also, MinDΔ10, which lacks the membrane targeting sequence, increases the toxicity of MinC, just not as well as the full-length MinD (Hu and Lutkenhaus, 2001). These results are consistent with MinD enhancing the affinity of $MinC^C$ for FtsZ, and/or performing some other function of which we are unaware.

The last 15–20 residues of FtsZ – a busy region for protein interactions

FtsZ is one of the most conserved proteins in bacteria, consistent with its critical role in cell division. It consists of a main body ($FtsZ_{1\text{-}320}$ in *E. coli*), which is structurally homologous to tubulin, and an unstructured tail ($FtsZ_{321\text{-}383}$ in *E. coli*), which is less conserved and shows significant variation in length and sequence (Lowe and Amos, 1998; Ma and Margolin, 1999) (Fig. 1). However, the last ~15 residues of this tail are highly conserved in FtsZ from bacteria, suggesting a conserved function for this region. Indeed, this tail is involved in interaction with FtsA and ZipA in *E. coli* and EzrA and SepF (YlmF) in *Bacillus subtilis* (Haney *et al*., 2001; Ishikawa *et al*., 2006; Singh *et al*., 2007). Here, we show that it is also involved in interacting with $MinC^C$/MinD and therefore MinC/MinD. The interaction with FtsA and ZipA is required for Z-ring formation, whereas the interaction with EzrA or MinC/

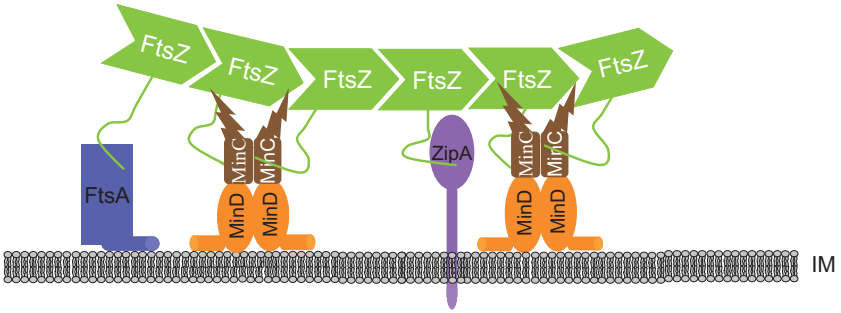

Fig. 8. Model for the inhibitory action of MinC/MinD on Z-ring assembly. Under physiological conditions polar Z-ring formation is prevented by MinC/MinD concentrated at the poles through the Min oscillation. MinC/MinD in the polar zone binds to ZipA and FtsA decorated FtsZ polymers located at the membrane before a complete Z ring is assembled through the MinC^{C}/MinD–FtsZ interaction. This binding may displace FtsA and/or ZipA from FtsZ polymers. More importantly the binding of MinC/MinD to FtsZ brings MinC^{N} close to FtsZ polymers, resulting in disruption of FtsZ polymers. The combination of these activities ensures that no polar Z rings are assembled. IM, inner membrane.

MinD has regulatory roles. Because this region is mediating interaction with many proteins, most of the mutants we isolated (D373E, I374V, L378V) result in small biochemical changes; the mutant proteins must still interact with other proteins (FtsA and ZipA) to function in division. Nonetheless, these subtle changes result in significant resistance to MinC/MinD and are deficient in MinC^{C}/MinD binding. The *ftsZ-I374V* mutation did not affect the interaction between FtsZ and ZipA; however, the interaction with FtsA was possibly reduced. Nonetheless, recruitment of FtsA to the Z ring appeared normal suggesting that there is still a strong enough interaction.

MinC^{C}/MinD disrupts the Z ring in two stages

It was shown previously that MalE-MinC^{C} inhibits the lateral association of FtsZ polymers *in vitro* and this activity was proposed to be the basis for the inhibitory activity of MinC^{C}/MinD *in vivo* (Dajkovic *et al.*, 2008a). Here we show that MinC^{C}/MinD blocks division in two stages. In the first stage MinC^{C}/MinD displaces FtsA from the Z ring. This requires less MinC^{C}/MinD but prevents the recruitment of downstream proteins such as FtsK. As a result the Z ring is non-functional for division. At the second stage, requiring more MinC^{C}/MinD, the Z ring is disrupted probably because ZipA is also displaced. The fact that MinC^{C}/MinD displaces FtsA more readily than ZipA could mean that FtsA binds the tail of FtsZ with lower affinity than ZipA or could simply be due to the Z ring containing less FtsA molecules than ZipA (ZipA/FtsA = 4/1). We don't have direct evidence to demonstrate that the eventual disintegration of the Z ring by MinC^{C}/MinD is due to the displacement of ZipA. It is possible that inhibition of the lateral association of FtsZ polymers by MinC^{C}/MinD is also a contributing factor.

The observation that the FtsA is displaced from the Z ring more readily than ZipA explains why the Z rings fail to function upon MinC^{C}/MinD induction. The Z rings persist with the aid of ZipA but do not function because FtsA, FtsK and presumably other cell division proteins are absent. A previous study (Justice *et al.*, 2000) concluded that MinC/MinD prevented the recruitment of FtsA to the Z ring instead of disrupting the Z ring to inhibit division. However, there are several studies showing that MinC/MinD does indeed disrupt the Z ring (Hu *et al.*, 1999; Pichoff and Lutkenhaus, 2001; Johnson *et al.*, 2002) and we find that the integrity of Z rings are much more sensitive to intact MinC/MinD than MinC^{C}/MinD. We cannot explain the difference between our results and their observations although they obtained different results depending upon the fixation conditions. It's possible that they had a mutation that inactivated the N terminus of MinC in their MinC/MinD construct, making it more or less like MinC^{C}/MinD. However, they also reported that overexpression of FtsA reduced the filamentation caused by their MinC/MinD construct but we were unable to find conditions where overexpression of FtsA (despite trying many different expression levels) reduced the filamentation caused by overexpression of MinC^{C}/MinD. This is perhaps not so surprising because expression of MinC^{C}/MinD at the minimal level required to cause uniform filamentation is unlikely to only displace FtsA but also starts to affect ZipA. Also, overexpression of FtsA would place more FtsA on the Z ring but this can be detrimental because the ratio of these proteins (FtsZ, FtsA, ZipA) must be within a certain window for the normal functioning of the Z ring (Dai and Lutkenhaus, 1992; Hale and de Boer, 1997).

Model for MinC/MinD on Z-ring formation

With the results obtained here and previous studies, we provide details that support a model for the mode of action of MinC/MinD in preventing formation of Z rings (Johnson *et al.*, 2004). As shown in Fig. 8, MinC/MinD localizes to membrane-associated FtsZ polymers through MinC^{C}/

MinD interacting with the conserved C-terminal tail of FtsZ. By directly contacting FtsZ, MinC/MinD prevents Z-ring formation in at least two ways: first, MinC^C/MinD disrupts the function of the Z ring by interfering with the recruitment of FtsA and possible reducing polymer bundling; second, this targeting of MinC/MinD to the Z ring brings MinC^N in close proximity to FtsZ polymers, so that it is near its target. The combination of these two activities makes MinC/MinD a potent division inhibitor.

The resistance of the FtsZ I374V mutant to MinC/MinD suggests that the targeting of MinC/MinD to the Z ring (through MinC^C/MinD) is very important for its activity; on the other hand the observation that the presence of the *ftsZ I374V* allele (BSZ374 strain) in a WT background (*min*$^+$) results in very few minicells almost argues against this. Comparison of the division inhibitory activity of the two domains of MinC (by employing mutations that inactivate either domain in the context of MinC/MinD) revealed that they have the same efficiency in blocking division and preventing colony formation. Each domain, however, is much less efficient than full-length MinC/MinD (Fig. 6), suggesting that the two parts of MinC work synergistically to achieve maximum activity. The importance of the two domains of MinC is further highlighted by the observation that the *min* operon containing the *minC-G10D* or the *minC-R172A* mutations on a single copy plasmid cannot prevent minicell formation (Zhou and Lutkenhaus, 2005; M. Wissel and J. Lutkenhaus, unpubl. results).

Why the FtsZ-I374V mutant does not make minicells is not clear. We think one possible reason is that, as we have shown, FtsZ-I374V is still sensitive to MinC^N. The presence of MinE in the cell concentrates MinC/MinD at the poles through the oscillation and the high polar concentration of MinC^N (as part of MinC) may disrupt the polar Z rings. Consistent with FtsZ-I374V being sensitive to MinC^N, we have shown that expression of MinC/MinD at a higher level prevents the growth of BSM374 (Fig. 6, row 3). However, this cannot be the only reason as we have shown in Fig. 6 that BSM374 (*ftsZ-I374V*, *min::kan*) has the same sensitivity to WT MinC/MinD as S4 (*ftsZ*-WT, *min::kan*) has to MinC-R172A/MinD. This result indicates that the two mutations (*ftsZ-I374V* and *minC-R172A*) are similar in affecting the responsiveness of FtsZ to MinC/MinD. Nevertheless, MinC-R172A cannot block minicell formation in FtsZ-WT strain (Zhou and Lutkenhaus, 2005) whereas WT MinC efficiently prevents minicell formation in FtsZ-I374V strain. We do not know what the basis is for the difference between these two cases. However, the fact that BSZ374 strain is not making minicells does not necessarily mean that the targeting of MinC/MinD to the Z ring is not required for its function at physiological levels (can be deduced from the effect of MinC-R172A). At overexpressed levels the two domains of MinC can function separately but combining them results in an inhibitor that works synergistically to ensure the disruption of polar Z rings. In this sense, it will be interesting to know whether minicells are formed if a MinC^N-resistant *ftsZ* allele is present on the chromosome.

Experimental procedures

Bacterial strains, plasmids and growth conditions

Strains and plasmids used in this study are listed in Table S3. Cells were grown in Luria–Bertani (LB) medium at 37°C unless otherwise indicated. When needed, antibiotics were used at the following concentrations: ampicillin = 100 μg ml^{-1}, spectinomycin = 25 μg ml^{-1}, kanamycin = 25 μg ml^{-1}, tetracycline = 10 μg ml^{-1}, cephalexin = 20 μg ml^{-1} and chloramphenicol = 20 μg ml^{-1}.

Strain S7 (*ftsZ*^{0}*recA*::Tn*10*)/pKD3C was constructed in two steps. First the *ftsZ*^{0} allele was introduced into strain S4 (*leu*::Tn*10* *ftsZ*$^+$*min::kan*)/pKD3C (*ftsZ*$^+$) with P1 phage grown on PB143 (*leu*$^+$*ftsZ*^{0}*recA*::Tn*10*) by selecting Leu$^+$ at 30°C on M9 minimal medium. The resultant transductants were checked for temperature and tetracycline sensitivity. The desired transductants (S6/pKD3C) should have the genotype of *leu*$^+$, *ftsZ*^{0}, *min::kan* with the temperature-sensitive plasmid pKD3C supplying FtsZ. In a second step, the *recA*::Tn*10* allele from PB143 was transduced into S6/pKD3C by selecting tetracycline resistance on LB plates at 30°C. The resultant cells S7 (*ftsZ*^{0}*recA::Tn10*)/pKD3C) were checked for UV sensitivity to confirm *recA* inactivation.

The strain BSZ374 (*ftsZ-I374V*) was generated by replacing the *ftsZ84* allele (TS) on the chromosome of strain PS106 with *ftsZ-I374V* through recombineering using the lambda RED system (Datsenko and Wanner, 2000). The PCR product of *ftsZ* containing the *I374V* mutation was electroporated into PS106 (*ftsZ84*)/pKD46 induced with arabinose = 0.04% for 3 h at 30°C and recombinants were selected on LB plates with no salt at 42°C. To determine if the *ftsZ-I374V* mutation was present, 10 colonies were randomly selected and checked for MinC/MinD resistance (about 25% of the randomly streaked colonies showed MinC/MinD resistance). We then did PCR to amplify the *ftsA-ftsZ* region from the chromosome of the MinC/MinD-resistant strains and confirmed that *ftsZ I374V* was present and that *ftsZ84* was absent. P1 transduction was then used to move the *min::kan* allele into BSZ374 to give BSM374.

The plasmid pBANG112 was constructed by inserting a fragment containing *ftsZ* into a pACYC184-based vector. The *ftsZ* gene was obtained by XmaI and PstI digestion of pKD4 (Dai and Lutkenhaus, 1991). To make pBANG59, *minC*/*minD* was PCR amplified from pSC104CD using primers (restriction sites underlined): 5′-MinC-SstI: GGAGCTCGCTAATTG AGTAAGGCCAGGATG and 3′-MinD- HindIII: CATGTCCT GCAGAAGCTTGCATTAAAATCTAGCGAGGGC. digested with SstI+HindIII and inserted to a Spc^r version of pEXT22. pBANG75 and pBANG78 were made by replacing *gfp-minC*^{C}/*minD* in pHJZ109 (Zhou and Lutkenhaus, 2005) with the properly digested *minC*^{C}/*minD* and *minC*/*minD* PCR product respectively. Both *minC*/*minD* and *minC*^{C}/*minD* were amplified from pCS104CD (Zhou and Lutkenhaus, 2005) using the following primers (restriction sites underlined): 5′-MinC*-SstI: CGAGCTCTTTAAGAAGGAGATATACGGATG

TCAAACACGCCAATCG; 5′-MinC^{C116}-SstI: CGAGCTCTA AGGAGGTTATAAATAATGGCGCAAAATACAACGCCGGTC and 3′-MinD- HindIII: CATGTCCTGCAGAAGCTTGCATTA AAATCTAGCGAGGGC. Both pBANG75 and pBANG78 contain artificially conserved ribosome binding site for MinC^{C} and MinC translation respectively.

PCR random mutagenesis of ftsZ

Using pBANG112 as the template and the primers: 5′-GC CTCAGGCGACAGGCACAAATCGGAGAG and 5′-GCTGC AGATATTCGATATCACGCATGAAAC, *ftsZ* was PCR amplified using the GeneMorph II Random Mutagenesis kit from Stratagene with a mutagenesis rate of 1–4 bases/kb. The PCR fragments were then digested with EcoRI+EagI and ligated into EcoRI+EagI-digested pBANG112. The ligation product was then electroporated into S7/pKD3C and transformants were selected at 42°C on plates with ampicillin. All colonies that grew up were pooled to give a library of FtsZ mutants that can still complement the *ftsZ* depletion strain and support cell division. Then pBANG75 was transformed into these cells and colonies resistant to MinC^{C}/MinD were selected with IPTG = 200 μM at 42°C on plates containing Amp and Spc. Plasmids were isolated from colonies that grew and the *ftsZ* gene was sequenced to identify the mutations.

Analysis of GFP–MinC^{C}/MinD localization

Overnight cultures of S4, BSM374 or JS964 (*min::kan*) containing the plasmid pHJZ109 (*gfp-minC^{C}minD*) were diluted 1000-fold into LB+Spc and grown at 37°C until $OD_{600} \approx 0.3$. IPTG was then added at the indicated concentrations and the cultures were diluted every 0.5–1 h to keep the $OD_{600} < 0.4$. Samples were taken at different time points and checked by microscopy as previously described (Zhou and Lutkenhaus, 2005).

Yeast two hybrid assay

To detect FtsZ–FtsA and FtsZ–ZipA interactions, the appropriate plasmids were transformed into the reporter strain SFY526 as described (Huang *et al*., 1996). The colonies obtained were analysed for β-galactosidase production by the colony lift assay described in the CLONTECH manual.

Protein purification and FtsZ recruitment assay

Wild-type FtsZ and FtsZ I374V were expressed and purified from W3110/pKD126 (*ftsZ*) and BSZ374/pKD126-1(*ftsZ-I374V*) respectively, according to the method described previously (Mukherjee and Lutkenhaus, 1998). A slight modification was that after ammonium sulphate precipitation, the pellet was dissolved and dialysed in Buffer A and further purified by chromatography on a Resource Q column (GE healthcare) eluting with 50 mM Tris-HCl (pH 7.9), 1 mM EDTA, 10% glycerol, and a gradient of 50–500 mM KCl. The FtsZ fractions (eluting at 200–300 mM KCl) were pooled and dialysed against 50 mM HEPES-NaOH (pH 7.2), 0.1 mM EDTA and 10% glycerol, aliquoted and stored at –80°C. The quality of the purified proteins was checked by sodium dodecyl sulphate polyacrylamide gel electrophoresis (SDS-PAGE) following the standard FtsZ polymerization assay (Dajkovic *et al*., 2008a). The purification of MalE-MinC^{C} and MinD and the FtsZ recruitment assay were performed as previously described (Dajkovic *et al*., 2008a).

Immunofluorescent microscopy

Overnight cultures of S4/pBANG75 and BSM374/pBANG75 were diluted 1000-fold in LB+Spc and grown at 37°C. At $OD_{600} \approx 0.3$, samples were taken and fixed with paraformaldehyde + glutaraldehyde. At the same time the cultures were diluted 10 times to fresh LB+Spc and induced with IPTG = 100 μM. Samples were taken and fixed every hour and cultures were diluted every hour to maintain the exponential phase. As a control, an exponentially growing culture of S4/pBANG75 was treated with 20 μg ml^{-1} cephalexin for 2 h and then cells were fixed with paraformaldehyde + glutaraldehyde. Fixation of the cells, preparation for immunostaining and photography of samples were done as described before (Pichoff and Lutkenhaus, 2002). The antisera were used at following concentrations: FtsZ (1/5000), FtsA (1/5000), ZipA (1/4000) and FtsK (1/1000).

Western blot

Strains grown in LB medium (supplemented with Spc if necessary and IPTG at indicated concentrations) included S3, S4, S4/pBANG59 (with IPTG = 40 μM), S4/pBANG78-G10D (with IPTG = 30 μM), S4/pBANG78-R172A (with IPTG = 30 μM), BSM374/pBANG78 (with IPTG = 25 μM) and BSM374/pBANG78-R172A (with IPTG = 40 μM) at 37°C for about 3 h to reach $OD_{600} = 0.4$. Cells are then collected and resuspended in SDS sample buffer, boiled for 10 min, and subjected to SDS-PAGE. Subsequent immunoblotting was done as previously described (Zhou and Lutkenhaus, 2005). For a better comparison, the loading volume for these samples is adjusted as follows: for S3, S4 and S4/pBANG59, the loading volume is equivalent to 300 μl of $OD_{600} = 0.4$ cells; for the others it is 60 μl of $OD_{600} = 0.4$ cells.

Acknowledgements

We thank Piet de Boer for sending strains. This work was supported by National Institutes of Health Grant GM029764.

References

Bernhardt, T.G., and de Boer, P.A. (2005) SlmA, a nucleoid-associated, FtsZ binding protein required for blocking septal ring assembly over chromosomes in *E. coli*. *Mol Cell* **18:** 555–564.

Bi, E., and Lutkenhaus, J. (1993) Cell division inhibitors SulA and MinCD prevent formation of the FtsZ ring. *J Bacteriol* **175:** 1118–1125.

Bi, E.F., and Lutkenhaus, J. (1991) FtsZ ring structure associated with division in *Escherichia coli*. *Nature* **354:** 161–164.

de Boer, P.A., Crossley, R.E., and Rothfield, L.I. (1989) A division inhibitor and a topological specificity factor coded for by the minicell locus determine proper placement of the division septum in *E. coli*. *Cell* **56:** 641–649.

de Boer, P.A., Crossley, R.E., and Rothfield, L.I. (1990) Central role for the *Escherichia coli minC* gene product in two different cell division-inhibition systems. *Proc Natl Acad Sci USA* **87:** 1129–1133.

Chen, Y., and Erickson, H.P. (2005) Rapid *in vitro* assembly dynamics and subunit turnover of FtsZ demonstrated by fluorescence resonance energy transfer. *J Biol Chem* **280:** 22549–22554.

Cordell, S.C., Anderson, R.E., and Lowe, J. (2001) Crystal structure of the bacterial cell division inhibitor MinC. *EMBO J* **20:** 2454–2461.

Dai, K., and Lutkenhaus, J. (1991) *ftsZ* is an essential cell division gene in *Escherichia coli*. *J Bacteriol* **173:** 3500–3506.

Dai, K., and Lutkenhaus, J. (1992) The proper ratio of FtsZ to FtsA is required for cell division to occur in *Escherichia coli*. *J Bacteriol* **174:** 6145–6151.

Dai, K., Mukherjee, A., Xu, Y., and Lutkenhaus, J. (1994) Mutations in *ftsZ* that confer resistance to SulA affect the interaction of FtsZ with GTP. *J Bacteriol* **176:** 130–136.

Dajkovic, A., Lan, G., Sun, S.X., Wirtz, D., and Lutkenhaus, J. (2008a) MinC spatially controls bacterial cytokinesis by antagonizing the scaffolding function of FtsZ. *Curr Biol* **18:** 235–244.

Dajkovic, A., Mukherjee, A., and Lutkenhaus, J. (2008b) Investigation of regulation of FtsZ assembly by SulA and development of a model for FtsZ polymerization. *J Bacteriol* **190:** 2513–2526.

Datsenko, K.A., and Wanner, B.L. (2000) One-step inactivation of chromosomal genes in *Escherichia coli* K-12 using PCR products. *Proc Natl Acad Sci USA* **97:** 6640–6645.

Ebersbach, G., Galli, E., Moller-Jensen, J., Lowe, J., and Gerdes, K. (2008) Novel coiled-coil cell division factor ZapB stimulates Z ring assembly and cell division. *Mol Microbiol* **68:** 720–735.

Fu, X., Shih, Y.L., Zhang, Y., and Rothfield, L.I. (2001) The MinE ring required for proper placement of the division site is a mobile structure that changes its cellular location during the *Escherichia coli* division cycle. *Proc Natl Acad Sci USA* **98:** 980–985.

Gueiros-Filho, F.J., and Losick, R. (2002) A widely conserved bacterial cell division protein that promotes assembly of the tubulin-like protein FtsZ. *Genes Dev* **16:** 2544–2556.

Hale, C.A., and de Boer, P.A. (1997) Direct binding of FtsZ to ZipA, an essential component of the septal ring structure that mediates cell division in *E. coli*. *Cell* **88:** 175–185.

Hale, C.A., and de Boer, P.A. (1999) Recruitment of ZipA to the septal ring of *Escherichia coli* is dependent on FtsZ and independent of FtsA. *J Bacteriol* **181:** 167–176.

Hale, C.A., Rhee, A.C., and de Boer, P.A. (2000) ZipA-induced bundling of FtsZ polymers mediated by an interaction between C-terminal domains. *J Bacteriol* **182:** 5153–5166.

Hale, C.A., Meinhardt, H., and de Boer, P.A. (2001) Dynamic localization cycle of the cell division regulator MinE in *Escherichia coli*. *EMBO J* **20:** 1563–1572.

Haney, S.A., Glasfeld, E., Hale, C., Keeney, D., He, Z., and de Boer, P. (2001) Genetic analysis of the *Escherichia coli* FtsZ.ZipA interaction in the yeast two-hybrid system. Characterization of FtsZ residues essential for the interactions with ZipA and with FtsA. *J Biol Chem* **276:** 11980–11987.

Hu, Z., and Lutkenhaus, J. (1999) Topological regulation of cell division in *Escherichia coli* involves rapid pole to pole oscillation of the division inhibitor MinC under the control of MinD and MinE. *Mol Microbiol* **34:** 82–90.

Hu, Z., and Lutkenhaus, J. (2000) Analysis of MinC reveals two independent domains involved in interaction with MinD and FtsZ. *J Bacteriol* **182:** 3965–3971.

Hu, Z., and Lutkenhaus, J. (2001) Topological regulation of cell division in *E. coli*. spatiotemporal oscillation of MinD requires stimulation of its ATPase by MinE and phospholipid. *Mol Cell* **7:** 1337–1343.

Hu, Z., Mukherjee, A., Pichoff, S., and Lutkenhaus, J. (1999) The MinC component of the division site selection system in *Escherichia coli* interacts with FtsZ to prevent polymerization. *Proc Natl Acad Sci USA* **96:** 14819–14824.

Hu, Z., Gogol, E.P., and Lutkenhaus, J. (2002) Dynamic assembly of MinD on phospholipid vesicles regulated by ATP and MinE. *Proc Natl Acad Sci USA* **99:** 6761–6766.

Hu, Z., Saez, C., and Lutkenhaus, J. (2003) Recruitment of MinC, an inhibitor of Z-ring formation, to the membrane in *Escherichia coli*: role of MinD and MinE. *J Bacteriol* **185:** 196–203.

Huang, J., Cao, C., and Lutkenhaus, J. (1996) Interaction between FtsZ and inhibitors of cell division. *J Bacteriol* **178:** 5080–5085.

Ishikawa, S., Kawai, Y., Hiramatsu, K., Kuwano, M., and Ogasawara, N. (2006) A new FtsZ-interacting protein, YlmF, complements the activity of FtsA during progression of cell division in *Bacillus subtilis*. *Mol Microbiol* **60:** 1364–1380.

Johnson, J.E., Lackner, L.L., and de Boer, P.A. (2002) Targeting of (D)MinC/MinD and (D)MinC/DicB complexes to septal rings in *Escherichia coli* suggests a multistep mechanism for MinC-mediated destruction of nascent FtsZ rings. *J Bacteriol* **184:** 2951–2962.

Johnson, J.E., Lackner, L.L., Hale, C.A., and de Boer, P.A. (2004) ZipA is required for targeting of DMinC/DicB, but not DMinC/MinD, complexes to septal ring assemblies in *Escherichia coli*. *J Bacteriol* **186:** 2418–2429.

Justice, S.S., Garcia-Lara, J., and Rothfield, L.I. (2000) Cell division inhibitors SulA and MinC/MinD block septum formation at different steps in the assembly of the *Escherichia coli* division machinery. *Mol Microbiol* **37:** 410–423.

Lackner, L.L., Raskin, D.M., and de Boer, P.A. (2003) ATP-dependent interactions between *Escherichia coli* Min proteins and the phospholipid membrane in vitro. *J Bacteriol* **185:** 735–749.

Li, Z., Trimble, M.J., Brun, Y.V., and Jensen, G.J. (2007) The structure of FtsZ filaments *in vivo* suggests a force-generating role in cell division. *EMBO J* **26:** 4694–4708.

Liu, Z., Mukherjee, A., and Lutkenhaus, J. (1999) Recruitment of ZipA to the division site by interaction with FtsZ. *Mol Microbiol* **31:** 1853–1861.

Lowe, J., and Amos, L.A. (1998) Crystal structure of the bacterial cell-division protein FtsZ. *Nature* **391:** 203–206.

Lutkenhaus, J. (2007) Assembly dynamics of the bacterial

MinCDE system and spatial regulation of the Z ring. *Annu Rev Biochem* **76:** 539–562.

Lutkenhaus, J., Sanjanwala, B., and Lowe, M. (1986) Overproduction of FtsZ suppresses sensitivity of lon mutants to division inhibition. *J Bacteriol* **166:** 756–762.

Ma, X., and Margolin, W. (1999) Genetic and functional analyses of the conserved C-terminal core domain of *Escherichia coli* FtsZ. *J Bacteriol* **181:** 7531–7544.

Meinhardt, H., and de Boer, P.A. (2001) Pattern formation in *Escherichia coli*: a model for the pole-to-pole oscillations of Min proteins and the localization of the division site. *Proc Natl Acad Sci USA* **98:** 14202–14207.

Mukherjee, A., and Lutkenhaus, J. (1998) Purification, assembly, and localization of FtsZ. *Methods Enzymol* **298:** 296–305.

Mulder, E., and Woldringh, C.L. (1989) Actively replicating nucleoids influence positioning of division sites in *Escherichia coli* filaments forming cells lacking DNA. *J Bacteriol* **171:** 4303–4314.

Pichoff, S., and Lutkenhaus, J. (2001) *Escherichia coli* division inhibitor MinCD blocks septation by preventing Z-ring formation. *J Bacteriol* **183:** 6630–6635.

Pichoff, S., and Lutkenhaus, J. (2002) Unique and overlapping roles for ZipA and FtsA in septal ring assembly in *Escherichia coli*. *EMBO J* **21:** 685–693.

Pichoff, S., and Lutkenhaus, J. (2005) Tethering the Z ring to the membrane through a conserved membrane targeting sequence in FtsA. *Mol Microbiol* **55:** 1722–1734.

Pichoff, S., and Lutkenhaus, J. (2007) Identification of a region of FtsA required for interaction with FtsZ. *Mol Microbiol* **64:** 1129–1138.

Raskin, D.M., and de Boer, P.A. (1999a) MinDE-dependent pole-to-pole oscillation of division inhibitor MinC in *Escherichia coli*. *J Bacteriol* **181:** 6419–6424.

Raskin, D.M., and de Boer, P.A. (1999b) Rapid pole-to-pole oscillation of a protein required for directing division to the middle of *Escherichia coli*. *Proc Natl Acad Sci USA* **96:** 4971–4976.

Rothfield, L., Taghbalout, A., and Shih, Y.L. (2005) Spatial control of bacterial division-site placement. *Nat Rev Microbiol* **3:** 959–968.

Shih, Y.L., Le, T., and Rothfield, L. (2003) Division site selection in *Escherichia coli* involves dynamic redistribution of Min proteins within coiled structures that extend between the two cell poles. *Proc Natl Acad Sci USA* **100:** 7865–7870.

Shiomi, D., and Margolin, W. (2007) The C-terminal domain of MinC inhibits assembly of the Z ring in *Escherichia coli*. *J Bacteriol* **189:** 236–243.

Singh, J.K., Makde, R.D., Kumar, V., and Panda, D. (2007) A membrane protein, EzrA, regulates assembly dynamics of FtsZ by interacting with the C-terminal tail of FtsZ. *Biochemistry* **46:** 11013–11022.

Wang, L., and Lutkenhaus, J. (1998) FtsK is an essential cell division protein that is localized to the septum and induced as part of the SOS response. *Mol Microbiol* **29:** 731–740.

Wang, X., Huang, J., Mukherjee, A., Cao, C., and Lutkenhaus, J. (1997) Analysis of the interaction of FtsZ with itself, GTP, and FtsA. *J Bacteriol* **179:** 5551–5559.

Yu, X.C., and Margolin, W. (1999) FtsZ ring clusters in min and partition mutants: role of both the Min system and the nucleoid in regulating FtsZ ring localization. *Mol Microbiol* **32:** 315–326.

Zhou, H., and Lutkenhaus, J. (2005) MinC mutants deficient in MinD- and DicB-mediated cell division inhibition due to loss of interaction with MinD, DicB, or a septal component. *J Bacteriol* **187:** 2846–2857.

Supporting information

Additional supporting information may be found in the online version of this article.

Please note: Wiley-Blackwell are not responsible for the content or functionality of any supporting materials supplied by the authors. Any queries (other than missing material) should be directed to the corresponding author for the article.

